JOINT INSTITUTE FOR NUCLEAR RESEARCH

FINAL REPORT ON THE INTEREST PROGRAMME

Experimental investigations of (n, α) reaction on fast neutrons using an ionization chamber

Supervisor:
Dr. Dr Igor Chuprakov

Student:
An Binh Le, Viet Nam
University of Science, VNU-HCM

Participation period:
February 13 – April 02, Wave 8

Dubna, 2023

1. Abstract

The field of nuclear engineering, in particular, for assessing radiation damage to structural materials of nuclear installations, the choice of technical materials in carrying out calculations in the development of new objects for nuclear energy, is very interesting in the study of (n, α) reactions on fast neutrons.

The results of the experiments are stored in nuclear large databases. According to the number of significant countries having nuclear technology, there are five such files or libraries. They are ENDF/B-VII (USA), JENDL-3.3 (Japan), JEFF-3.0 (EU), CENDL-3 (China), and BROND-3 (Russia).

For many nuclei that are part of structural materials, the current state of affairs with theoretical estimates of the cross section (n, α) of the reaction given in various nuclear data libraries (ENDF / B-VII, JENDL-4.0, BROND 3 and others) is also unsatisfactory, and the scatter of the values of the estimated cross sections exceeds 20-30%.

The project's goal is to create and master a method for measuring the reaction cross section (n, α) on a variety of isotopes for fourth-generation nuclear-physical data libraries.

2. Introduction

Studies of neutron-induced reactions with the emission of charged particles are important for nuclear physics and technology. Therefore, experimental studies of this reaction can improve the existing library of nuclear data and can be used to test appropriate nuclear reaction models.

For investigating the primary source of neutrons to carry out further study, especially one of the main channels for the neutron-induced reaction. The reaction D(d, n)^{3}He was chosen to be the fast neutrons source using a deuterium gas and a deuterium/titanium solid target bombarded by an accelerated deuteron beam. Instead of having a practical experiment set up, an installation of EnergySet program is needed to gain data from the reaction. Therefore, the information on neutron energy, neutron flux, and the dependence of those on the emission angle with the cross section of reaction was studied readily. The interface of the simulation program is shown in Figure 1.

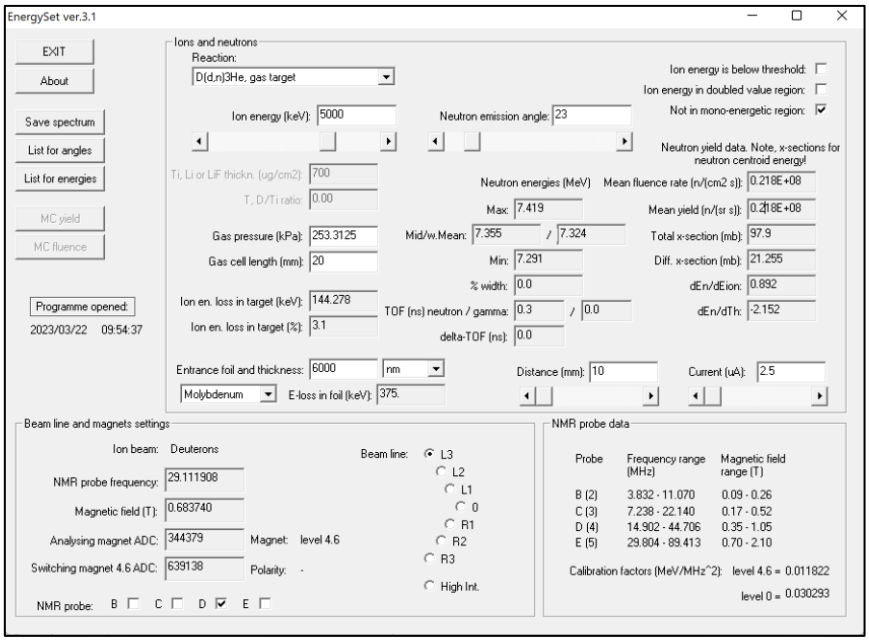

Fig. 1 *The interface of EnergySet simulation program.*

Program EnergySet was programmed by Göran Lövestam, one of the members of EC-JRC-IRMM locates at Retieseweg 111, Geel, Belgium and it was first released in Jan-2002. The file structure of EnergySet (Jan-2004) is shown in Table 1,

Table 1 *EnergySet main directory contents*

File	Function
EnergySet.exe	Executable file
EnergySetInp.txt	Input data file with input data
Reactions.txt	Input data file with included nuclear reactions and associated data
react_xx.txt	Input data files with cross section data
StoppingData.txt	Input data file with ion stoping data
AngleScan.txt	Input data file with angles and delays for scannded fluencies
qplot.txt	Output file containing momentarily updated neutron fluence spectrum
Spectr yyyymmdd hhmmss.txt	Output file giving neutron fluence as function of neutron energy
Angles yyyymmdd hhmmss.txt	Output file giving neutron fluence as function of neutron emission angle
Energy yyyymmdd hhmmss.txt	Output file giving neutron fluence as function of ion energy

3. Experiment methods

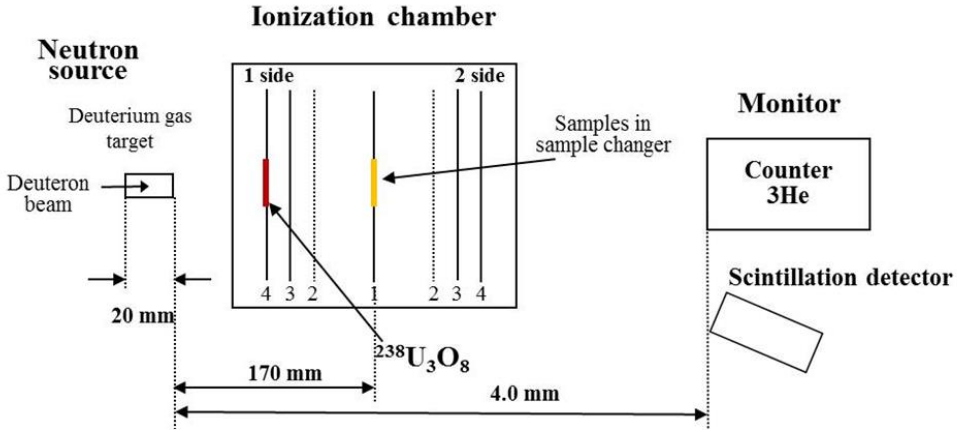

Fig. 2 *Experimental set up scheme. 1, 2, 3-common cathode with samples, grids, and anodes of the gridded twin ionization chamber (GIC), respectively; 4-fission chamber (FC) cathode.*

The experiments were carried out at the Frank Laboratory of Neutron Physics, Joint Institute for Nuclear Research, Russia (FLNP JINR) using the EG-5 Van de Graaff accelerator. Figure 2 depicts the experiment's setup, which consists of three parts: The neutron source, the twin gridded ionization chamber (GIC), and the ^{3}He counter. And the practical set up of the GIC device is shown in Figure 3.

3.1. Neutron source

Fast neutrons were produced via the D(d, n)^{3}He reaction alternatively using a deuterium gas target and deuterium doped with titanium solid target, the characteristic of two targets is shown in Table 2. The gas cylinder vessel 2.0 cm in length and 0.9 cm in diameter separated from the vacuum tube of the accelerator by molybdenum foil 6.0 μm in thickness. The pressure of the deuterium gas was 253.3 kPa, and the incident deuterium beam current was approximately 2.5 μA. The energy range of the incident deuterons was 1.2–5.2 MeV to generate neutrons with an energy range of 2.6–7.9 MeV.

3.2. Charge particle detector

The twin gridded ionization chamber (GIC) composed of two symmetric sections with a common cathode, supplemented by a fission chamber, is used as a charged particle detector. The shape of the chamber is cylindrical, with a diameter 28.2 cm and a height 27.2 cm, and the thickness of the stainless-steel wall is 2.0 mm. The distances

between the GIC electrodes were as follows: Cathode-grid 6.1 cm, grid-anode 1.8 cm, FC anode-cathode 1.0 cm. The distance from the edge of the deuterium target to the cathode of the GIC was 15.4 cm. Kr + 4% CH4 and Kr + 3% CO_2 were used as the working gas at a pressure of 1.3 atm, so the alpha particles can be stopped before reaching the grids.

There is a specially designed sample changer attached to the common cathode of the ionization chamber with five sample positions and two back-to-back samples can be placed at each of them. With the sample changer, it is convenient to change samples without opening the chamber. The two back-to-back samples were set at the first position of the sample changer for foreground measurement. α events in the forward (0^o–90^o) and backward (90^o–180^o) directions were measured simultaneously, therefore, the detection solid angle is almost 4π. Two samples of $^{238}U_3O_8$, with the 99.999% abundance, $N_U = 1.74\times10^{19}$ and $N_U = 1.5\times10^{19}$, are used for measurement of the absolute and relative neutron flux, placed on the sample changer and the fission cathode, respectively.

a) *b)*

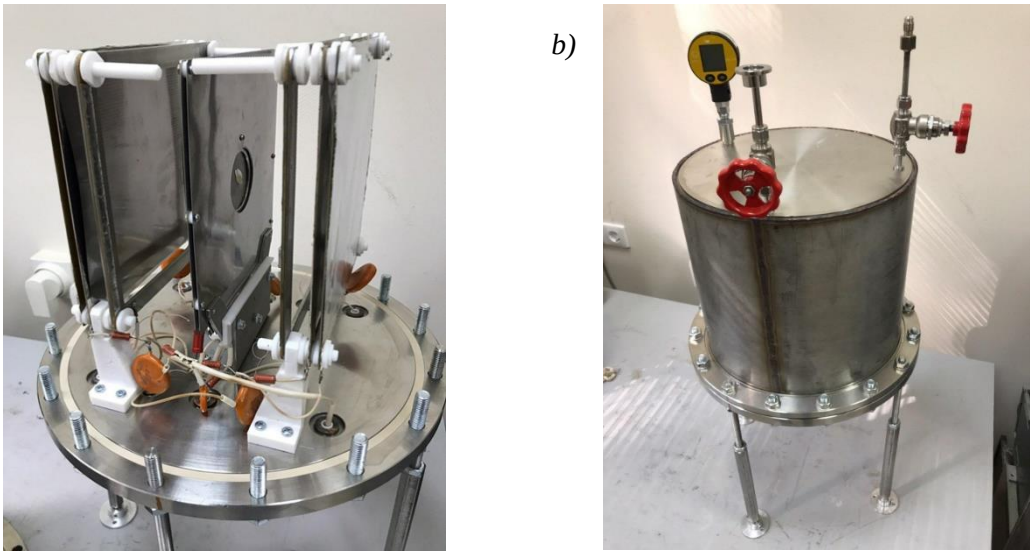

Fig. 3 *The practical GIC arrganement for the deuterium gas target. a) The core of the GIC with the round shaped sample changer among the grids. b) Ionization chamber is sealed while operating for keeping the gas pressure as desired.*

The grid electrodes were grounded, the high voltage applied to the anodes was +1000 V, and to the cathode −1500 V to collect the electrons from ionization completely. The cathode and anodes were covered with tantalum foil to reduce the

background. The detector signals were recorded using a 14-bit Pixie-16 module with a sampling frequency of 250 MHz. The Pixie system consists of a chassis (PXI-6023 XIA 14, Wiener), an embedded controller (NI PXI-8820), and a high-speed digitizer (Pixie-16) which is shown in Figure 4.

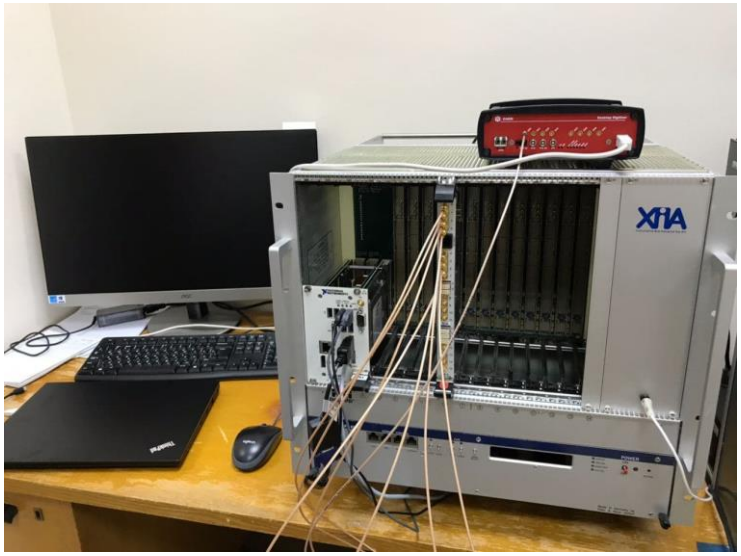

Fig. 4 *Data acquistion system*

Table 2 *Some characteristics of two targets.*

Solid target, D/Ti	Copper has been used as substrate, because of its high thermal conductivity. Its dimension is 20 and 2 mm in diameter and thickness, respectively. Its diameter is the same as of target holder diameter in the our neutron generators. Titanium (m = 1μg/cm^2) has been deposited on copper substrate by using ion coating method. These equipments are shown in Figure 5 with comparing to regular object.
Gas target, D_2	L (target) – 20 mm, P ~ 1 – 3 atm, I_d ~ 3-5 μA, l = 150 mm, d (Mo) ~ 6 μm, Φ_n ~ 107 1/c.

a)

b)

Fig. 5 *a) Titanium is placed on the copper substrate plates by ion coating procedure. b) Different diameters of the target holders.*

Fig. 6 *Expermental set up completion*

4. Result and discussion

4.1. Gas target (D_2)

The parameters of the EnergySet program were set to get mono-energetic fast neutrons were through the D(d,n)^{3}He reaction using a deuterium gas target bombarded by an accelerated deuteron beam. The beam current was about 2.5 μA. The deuterium gas cell, 20 mm in length and 0.9 cm in diameter, was separated from the vacuum tube through a molybdenum film 6.0 μm in thickness. The deuterium gas pressure was 2.5 atm during the simulation. The energy of the accelerated deuterons in the beam before entering the molybdenum film was 1.2-5.2 MeV.

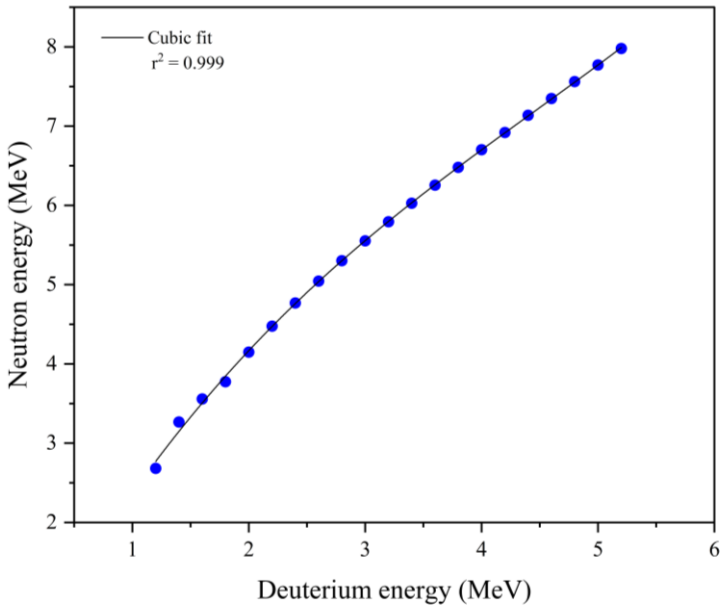

Fig. 7 *Relation between deuterium and neutron energy as the production from the reaction.*

As shown in Figure 7 the neutron energy from the reaction is proportional to deuterium energy, which is increasing as the deuterium energy increasing and it has the value from 2.6 to 7.9 MeV. The strong correlation between the incident deuterium energy and neutron energy ($r^2 = 0.999$) was found as a third order polynomial function, the value of fitting parameters is shown in Table 3,

$$E_n = aE_d^3 + bE_d^2 + cE_d + d \quad (1)$$

Tabel 3 *The value of parameters from fitting data*

Parameter	a	b	c	d
Value	0.02784	-0.37174	2.71728	-0.00249

With the neutron energy, the program also gives the mean neutron flux for corresponding incident deuterium energy. First, the correlation is studied without the dependence of the neutron emission angle (0^o).

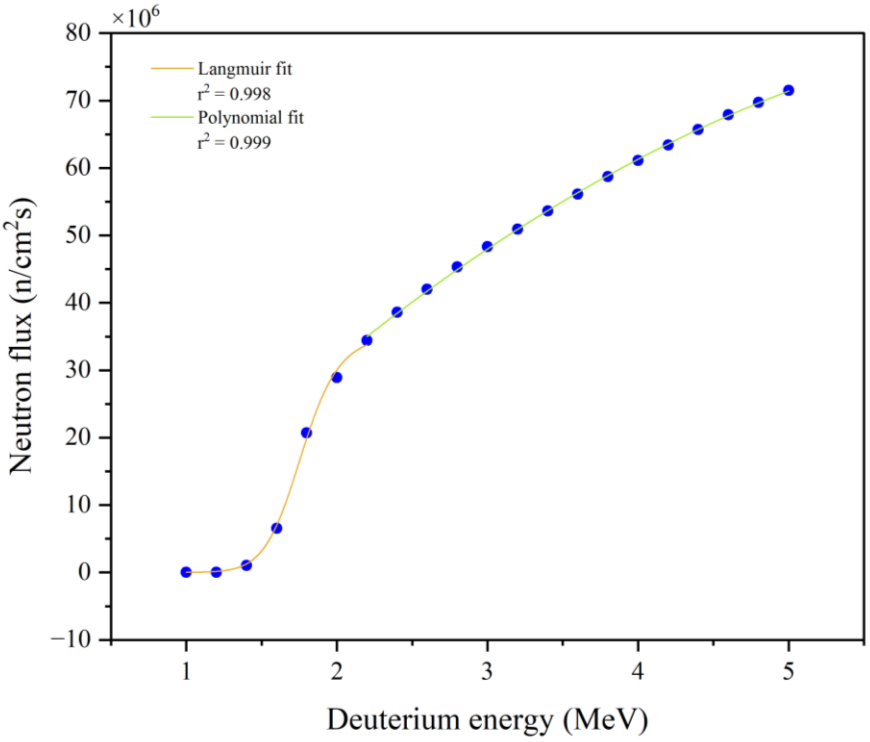

Fig. 8 *Relation between deuterium energy and neutron flux at 0^o neutron emission angle.*

The correlation between deuterium energy and the neutron flux was depicted using two separate functions, which are langmuir and polynomial for the deuterium energy range of 1.2-2.4 MeV and 2.4-5.2 MeV, respectively. These used functions are picked based on the optimal condition for the goodness of fit. The value of the fit parameters is shown in Table 4,

Langmuir function:

$$\phi_n = \frac{abE_d^{1-c}}{1+bE_d^{1-c}} \tag{2}$$

Polynomial function:

$$\phi_n = aE_d^2 + bE_d + c \quad (3)$$

Table 4 *The value of parameters from fitting deuterium energy and neutron flux*

Function	Range (MeV)	Parameters		
		a	b	c
Langmuir	1.2-2.4	3.52817×10^{7}	3.2621×10^{-4}	-13.10136
Polynomial	2.4-5.2	-16.00274×10^{5}	2.45255×10^{7}	-1.12109×10^{7}

Figure 9 shows the increase of the neutron flux at multiple neutron energy. According to the literature, the neutron energy decreases rapidly as the increasing of deuterium energy. Despite the horizontal line of the 1.2 MeV deuterium seeming to have zero neutron flux, the neutron flux at this deuterium energy has a significantly small value compared to other deuterium energy.

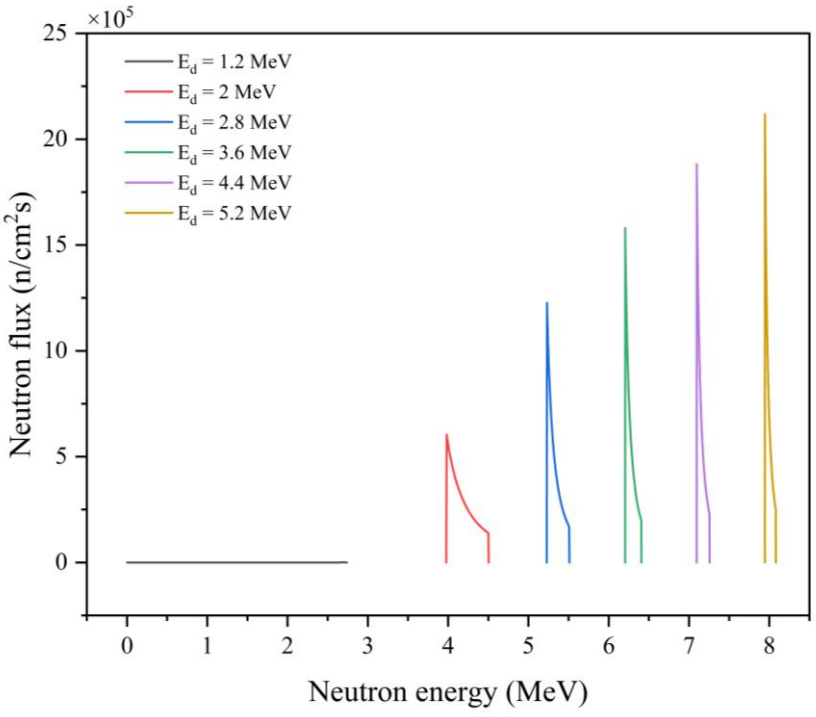

Fig. 9 *Comparison between neutron flux at different neutron energy for corresponding deuterium energy.*

The same as the deuterium energy and neutron flux, neutron energy and neutron flux was also fitted to find the correlation between them. Function (2) was used for the

regression of neutron energy from 2.7 to 4.5 MeV, the latter is fitted with function (3). Fitting parameter values are shown in Table 5.

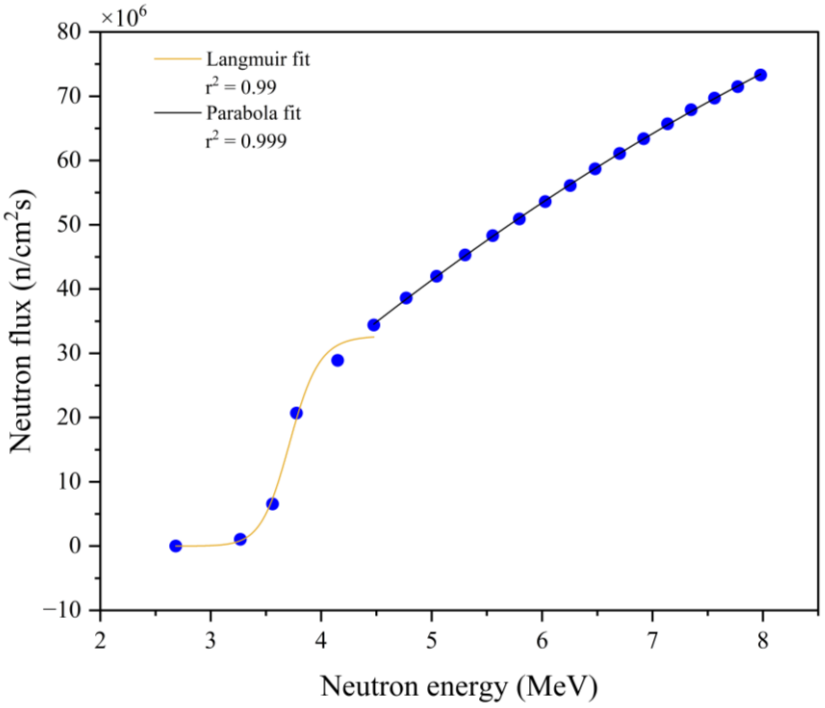

Fig. 10 *Relation between neutron energy and neutron flux.*

In Figure 10, neutron fluxes generally increase with rising neutron energy. At the energy range of 4.4-7.9 MeV, the neutron fluxes almost linearly increase with the neutron energy. However, the parabola function gives the best fit of the two data for this energy region (r^2 = 0.999). The neutron flux increase significantly in the 2.6-4.4 MeV span and that variety is best represented by langmuir function with a strong correlation (r^2 = 0.99).

Table 5 *The value of parameters from fitting neutron energy and neutron flux*

Function	Range (MeV)	Parameters		
		a	b	c
Langmuir	2.6-4.4	3.27135×10^{7}	1.04072×10^{-4}	-27.01989
Polynomial	4.4-7.9	-3.82846×10^{7}	1.91744×10^{7}	-648049.72237

The dependence of neutron fluxes on emission angles is also studied based on the simulation results of the EnergySet program. These data are shown in Figure 8 for a

variety of energy of incident deuterium from 1.2 to 5.2 MeV, with the change of neutron emission angle in the range of 10º-170º.

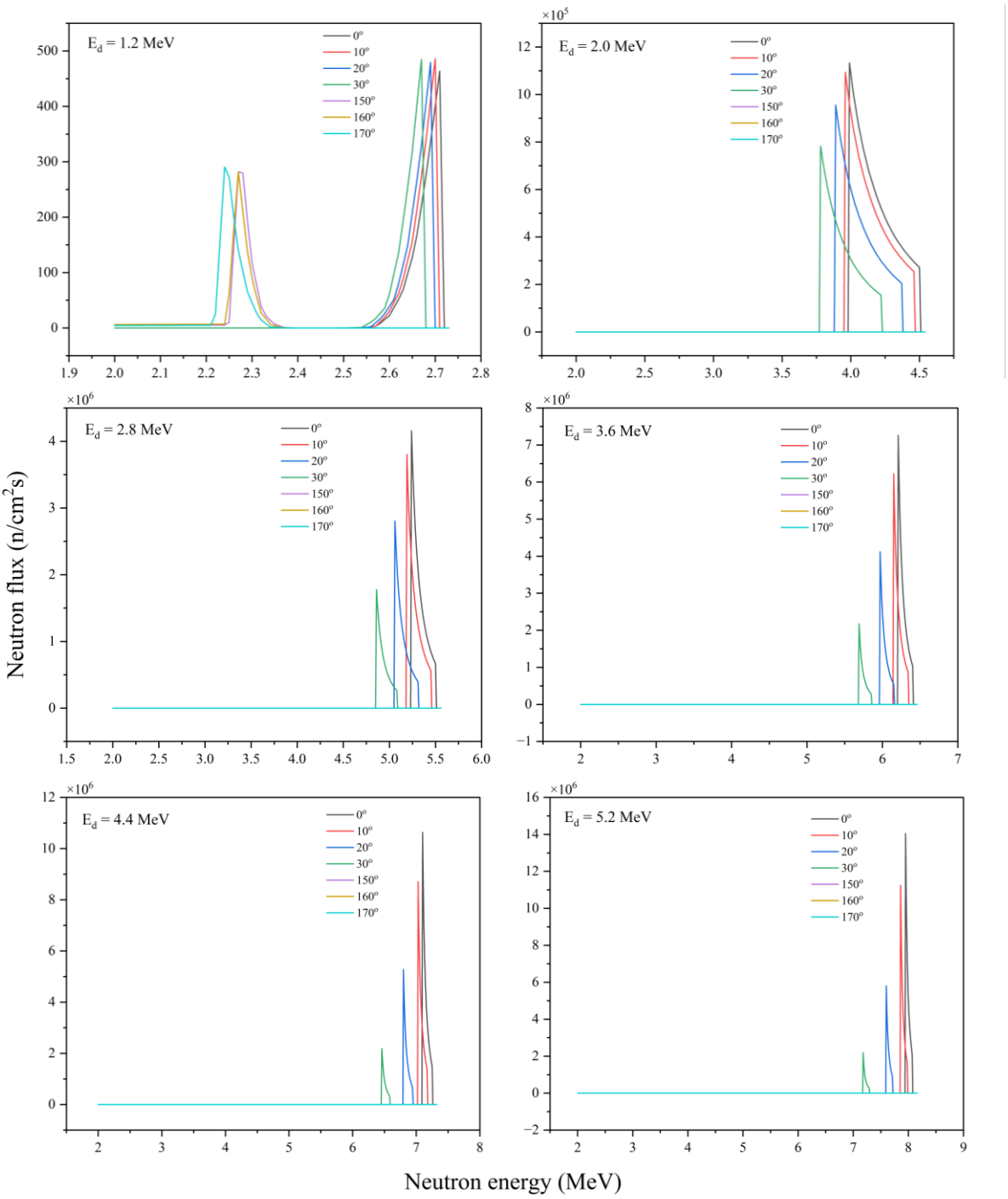

Fig. 11 *Comparison between different incident deuterium energy and neutron flux, which varies on the changing of neutron emission angle.*

It can be seen from Figure 11 that for the increasing energy of the incident deuterium, neutron energy, and neutron flux are also increasing. As was predicted in Figure 10 at 0º angle instance but the angle in Figure 11 has a wider studied range. For

the 1.2 MeV incident deuterium, the graph shows two distributions having approximately the same value. The first distribution locates at about 2.25 MeV neutron energy, having large emission angles, which are 150^{o}, 160^{o,} and 170^{o}. These angles have the neutron flux 281.79, 281.89, 290.44 n/cm^{2}s, respectively. The second distribution locates at around 2.65 MeV neutron energy with the smaller emission angles, these are 0^{o}, 10^{o}, 20^{o}, and 30^{o}. And they have the flux 463.52, 486.06, 479.18, and 484.82 n/cm^{2}s, respectively. For the other deuterium energy, at the neutron energy above 2 MeV, there are only four angles shown in the graph with the arrangement from smaller to higher flux values. These angles are 30^{o}, 20^{o}, 10^{o}, 0^{o}. Additionally, the decreasing rate of neutron flux becomes more dramatic when come to increasing deuterium energy with the same angle. This behavior appears more clearly when comparing neutron flux at 2 MeV deuterium energy of a specific angle to that one at 5.2 MeV deuterium energy.

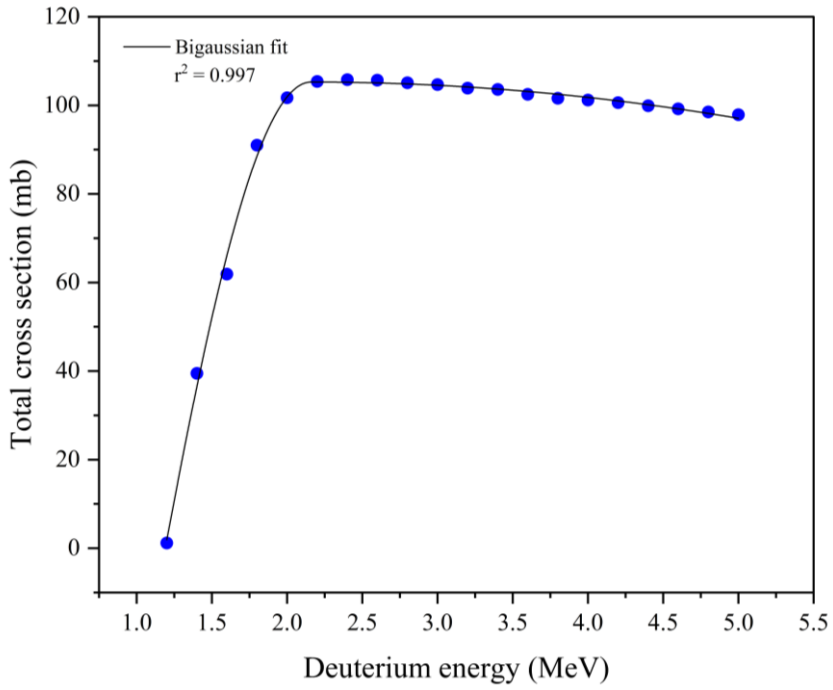

Fig. 12 *Relation between deuterium energy and total cross section.*

With the increase in incident deuterium energy, the cross section of the reaction is also dramatically increasing in the range of 1.2-2 MeV, which is shown in Figure 12. Otherwise, the cross section appears slightly decrease from 2 to 5.2 MeV deuterium energy. The correlation between deuterium energy and total cross section is also fitted using bigaussian function to demonstrate the regression,

Bigaussian function,

$$y = y_0 + He^{-0.5\left(\frac{x-x_c}{w_1}\right)^2} \qquad (x < x_c)$$
$$y = y_0 + He^{-0.5\left(\frac{x-x_c}{w_2}\right)^2} \qquad (x \geq x_c) \qquad (4)$$

Table 6 *The value of parameters from fitting deuterium energy and total cross section*

Parameters	y_0	x_c	H	w_1	w_2
Value	-251.32513	2.15879	356.58249	1.15928	13.18901

4.2. Solid target (D/Ti)

The majority of EnergySet program parameters set for a solid target are the same as the gas target but it has some adjustments. Instead of having gas pressure and gas cell length, the Ti thickness was set to 700 µg/cm^2 and value of the D/Ti ratio was 1.5. The other parameters and procedures were kept unchanged.

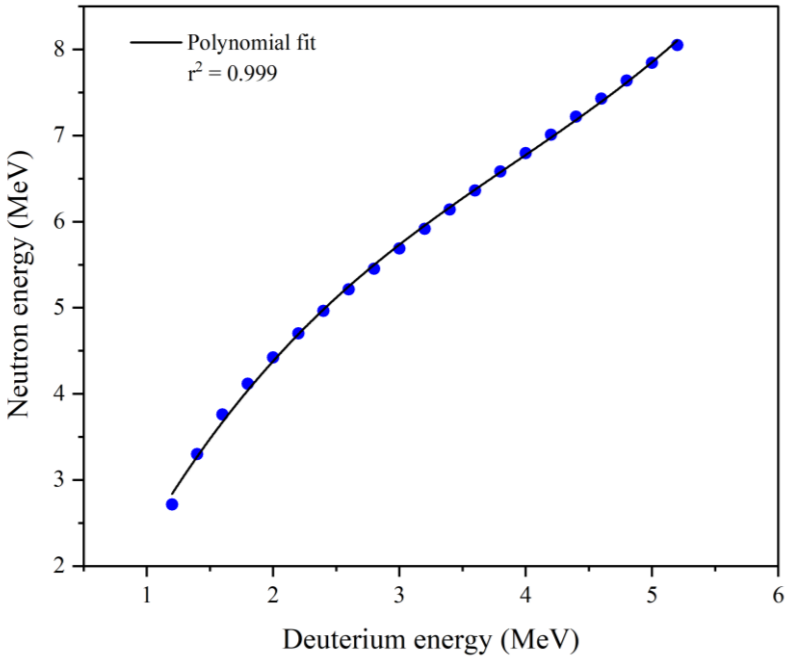

Fig. 13 *Relation between deuterium energy and neutron energy.*

As shown in Figure 13 the neutron energy from the reaction is proportional to deuterium energy, which is increasing as the deuterium energy increasing and it has the

value from 2.7 to 8.0 MeV. The strong correlation between the incident deuterium energy and neutron energy (r^2 = 0.999) was found by function (1), the value of fitting parameters is shown in Table 7,

Table 7 *The value of parameters from fitting data*

Parameters	a	b	c	d
Value	0.05792	-0.67728	3.63955	-0.65432

With the neutron energy, the program also gives the mean neutron flux for corresponding incident deuterium energy. First, the correlation is studied without the dependence of the neutron emission angle (0^o).

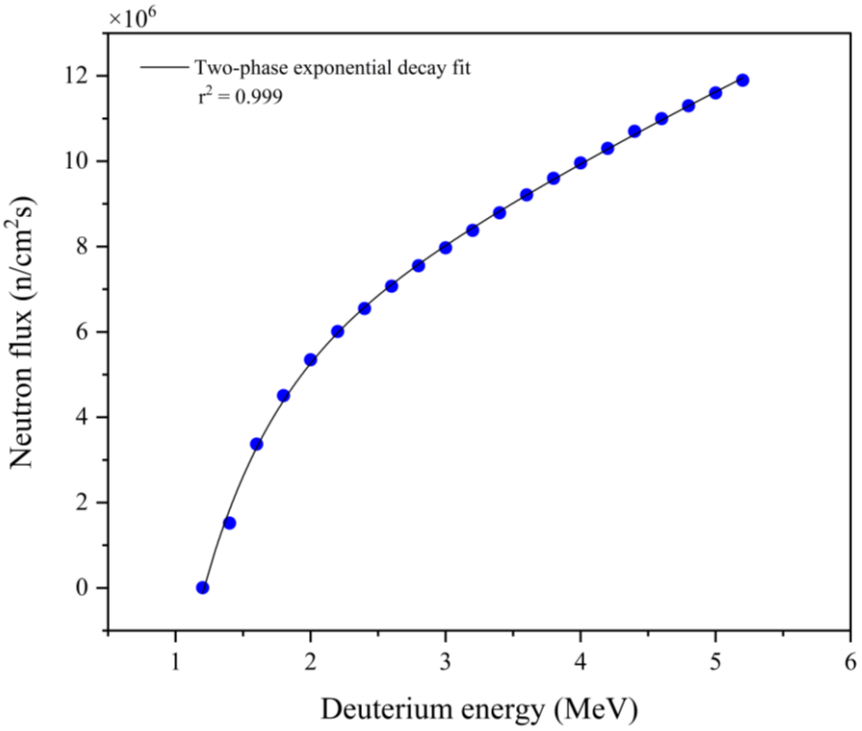

Fig. 14 *Relation between deuterium energy and neutron flux at 0^o neutron emission angle.*

The correlation between deuterium energy and the neutron flux was depicted using a two-phase exponential function. The used function is picked based on the optimal condition for the goodness of fit. The value of the fit parameters is shown in Table 8,

Two-phase exponential function,

$$y = y_0 + A_1 e^{-x/t_1} + A_2 e^{-x/t_2} \quad (5)$$

Table 8 *The value of parameters from fitting data*

Parameters	y_0	A_1	t_1	A_2	t_2
Value	3.6831×10^{7}	-4.9978×10^{7}	0.5100	-3.4783×10^{7}	15.5189

Figure 15 shows the increase of the neutron flux at multiple neutron energy. According to the literature, the neutron energy decreases rapidly as the increasing of deuterium energy. Despite the horizontal line of the 1.2 MeV deuterium seeming to have zero neutron flux, the neutron flux at this deuterium energy has a significantly small value compared to other deuterium energy.

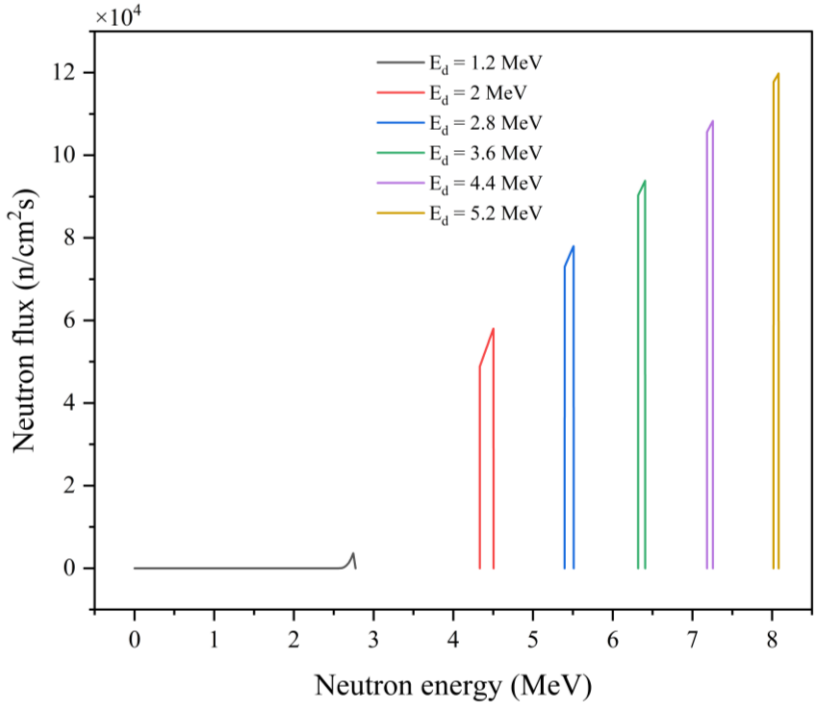

Fig. 15 *Comparison between neutron flux at different neutron energy for corresponding deuterium energy.*

Unlike gas target, Figure 15 shows that solid target yields increasing neutron flux for each deuterium energy. At the 1.2 MeV deuterium energy, the neutron flux has a span of a wide neutron energy range from 0 to 2.8 MeV, mostly with values of 10^{-7}-10^{-5} degrees of magnitude. It is very small when compared to neutron flux at other deuterium energy.

The same as the deuterium energy and neutron flux, neutron energy and neutron flux was also fitted to find the correlation between them. Function (1) was used for the regression of neutron energy from 2.7 to 8.0 MeV. Fitting parameter values are shown in Table 9.

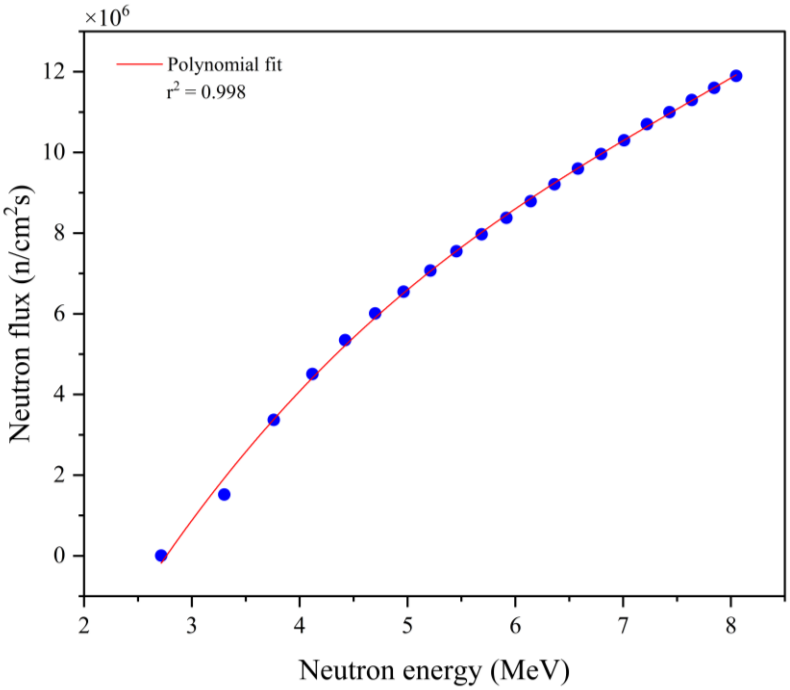

Fig. 16 *Relation between neutron energy and neutron flux.*

The graph in Figure 16 presents data on neutron fluxes increasing with rising neutron energy. In the low neutron energy region, neutron fluxes have discrete values and become denser in the higher energy region.

Table 9 *The value of parameters from fitting data*

Parameters	a	b	c	d
Value	30935.83753	-716340.42562	7072201.47466	-1.47245×10^{7}

The dependence of neutron fluxes on emission angles is also studied based on the simulation results of the EnergySet program for D/Ti target. These data are shown in Figure 17 for a variety of energy of incident deuterium from 1.2 to 5.2 MeV, with the change of neutron emission angle in the range of 10^{o}-170^{o}.

It can be seen from Figure 17 that for the increasing energy of the incident deuterium, neutron energy, and neutron flux are also increasing. As was predicted in Figure 14 at 0^o angle instance but the angle in Figure 17 has a wider studied range. For

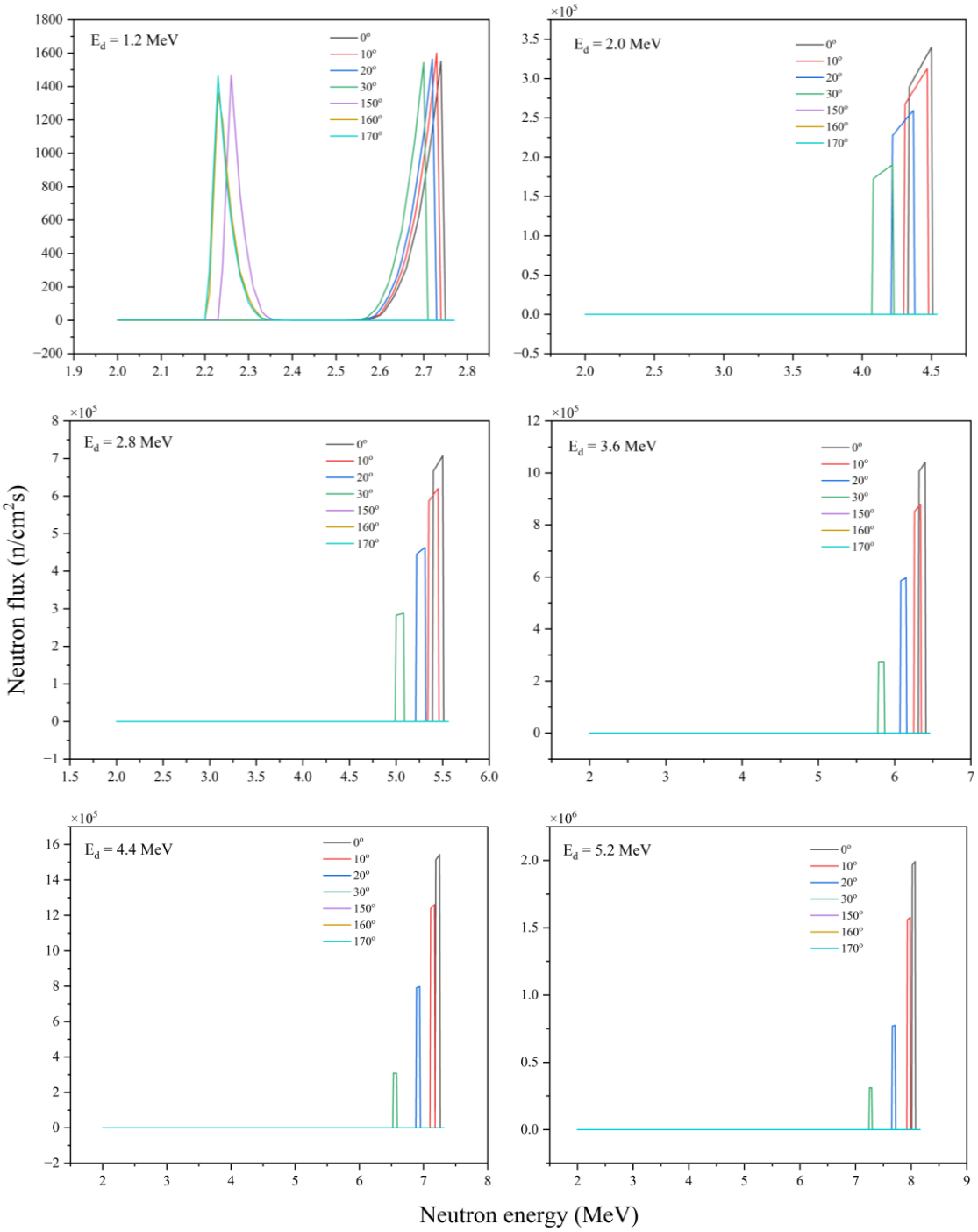

Fig. 17 *Comparison between different incident deuterium energy and neutron flux, which varies on the changing of neutron emission angle.*

the 1.2 MeV incident deuterium, the graph shows two distributions having approximately the same value. The first distribution locates at about 2.25 MeV neutron

energy, having large emission angle peaks, which are 150°, 160°, and 170°. These angle peaks have the neutron flux 1468.8, 1362.4, 1461.0 n/cm^{2}s, respectively. The second distribution locates at around 2.70 MeV neutron energy with the smaller emission angle peaks, these are 0°, 10°, 20°, and 30°. And they have the flux 1549.8, 1600.5, 1563.8, and 1543.8 n/cm^{2}s, respectively. For the other deuterium energy, at the neutron energy above 2 MeV, there are only four angles shown in the graph with the arrangement from smaller to higher flux values. These angles are 30°, 20°, 10°, 0°. Additionally, the increasing rate of neutron flux is hard to observe when comes to increasing deuterium energy with the same angle. This behavior appears more clearly when comparing neutron flux at 2 MeV deuterium energy of a specific angle to that one at 5.2 MeV deuterium energy.

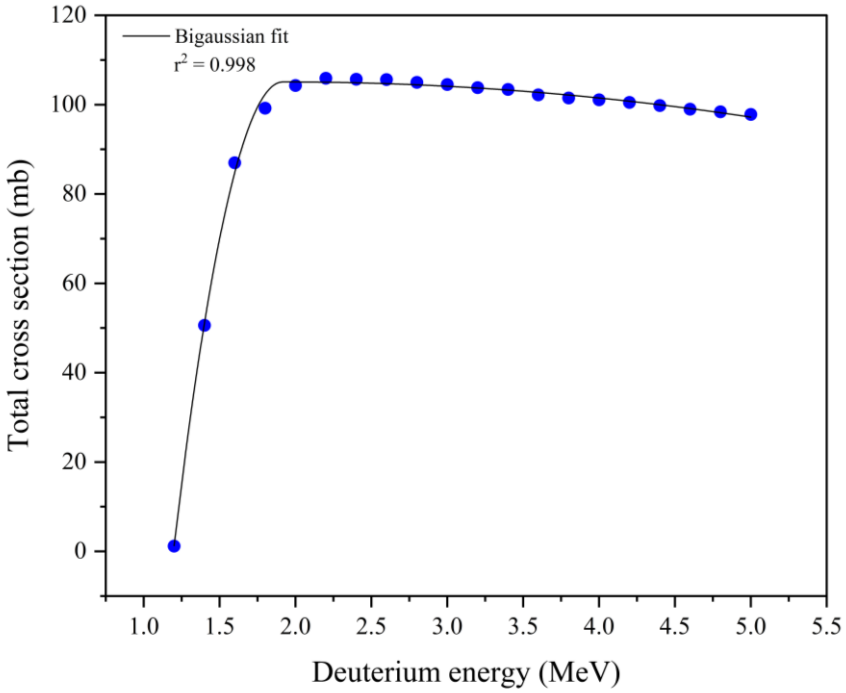

Fig. 18 *Relation between deuterium energy and total cross section.*

With the increase in incident deuterium energy, the cross section of the reaction is also dramatically increasing in the range of 1.2-2 MeV, which is shown in Figure 9. Otherwise, the cross section appears slightly decrease from 2 to 5.2 MeV deuterium energy. The correlation between deuterium energy and total cross section is also fitted using function (4) to display the regression. The value of fitting parameters is shown in Table 10.

Table 10 *The value of parameters from fitting deuterium energy and total cross section*

Parameters	y_0	x_c	H	w_1	w_2
Value	-41212.9779	1.91663	41318.06726	10.10325	157.97813

5. Conclusion

The D(d, n)^{3}He fusion reaction was investigated by using EnergySet simulation program, the energy range of incident deuterium was 1.2-5.2 MeV with 200 keV steps for both gas and solid target. In the instance of D_2 gas target, the gas pressure and the gas cell length were set to 2.5 atm and 20 mm, respectively. The D/Ti solid target thickness is specified at 700 μg/cm^2 with the ratio between D and Ti set to 1.5. The other parameters were kept unchanged for both targets, which are entrance foil and thickness, distance and current have the value of 6000 nm, 10 mm, 2.5 μA, respectively.

It shows that the simulation results indicate an increasing trend for the neutron energy as well as the neutron flux when incident deuterium energy becomes higher. The simulation gives the neutron energy in a range of 2.6-7.9 MeV for gas target, and with the solid target, the deuterium yields neutron energy 2.7-8.0 MeV. For deuterium energy above 2 MeV, the neutron flux of small angles (0^o, 10^o, 20^o, 30^o) is dominant at neutron energy above 2 MeV. Also above 2 MeV deuterium energy, the neutron flux tends to decrease at a specific angle for a gas target, this property is the opposite for a solid target. At 1.2 MeV deuterium energy, neutron fluxes appear to have two groups having approximately the same value. One group comprised larger emission angles (150^o, 160^o, 170^o) locate at about 2.25 MeV neutron energy, the other was made up of smaller angles (0^o, 10^o, 20^o, 30^o) at around 2.65 MeV neutron energy.

The cross section of the D(d, n)^{3}He reaction was simulated for the corresponding range of deuterium energy, and it has the highest value at 105.8 mb for 2.4 MeV deuterium energy of the gas target. With a solid target, the value is 105.9 mb at 2.2 MeV deuterium energy. All the correlated data were fitted using different functions and it shows a strong agreement between them.

6. Acknowledgements

I would like to thank INTEREST program for the organization of this project and the opportunity to gain new knowledge and experience. I also thank my supervisor Dr Igor Chuprakov for his help and support in the working of the project.

7. Reference

[1] Guohui Zhang, E. Sansarbayar, Yu. M. Gledenov, G. Khuukhenkhuu, L. Krupa, N. S. Gustova, M. G. Voronyuk, I. Chuprakov, N. Battsooj, I. Wilhelm, M. Solar, R. Sykoram, Z. Kohout, Jie Liu, Yiwei Hu, and Zengqi Cui «Cross sections of the ^{91}Zr(n, α)^{88}Sr reaction in the 3.9–5.3 MeV neutron energy region. Physical Review C 106, 064602, 2022.

[2] Haoyu Jiang, Zengqi Cui, Yiwei Hu, Jie Liu, Haofan Bai, Jin-Xiang Chen, Guo-Hui Zhang, Yu. M. Gledenov, E. Sansarbayar, G. Khuukhenkhuu, L. Krupa, I. Chuprakov, xichao ruan, Hanxiong Huang, Jie Ren and Qiwen Fan «Cross-section measurements for the 58,60,61Ni(n, α)55,57,58Fe reactions at 8.50, 9.50 and 10.50 MeV neutron energies», Chinese Physics C, 2021.

[3] E. Sansarbayar, Yu. M. Gledenov, I. Chuprakov, G. Khuukhenkhuu, G. S. Ahmadov, L. Krupa, Guohui Zhang, Haoyu Jiang, Zengqi Cui, Yiwei Hu, Jie Liu, N. Battsooj, I. Wilhelm, M. Solar, R. Sykora, and Z. Kohout «Cross sections for the 35Cl(n, α)32P reaction in the 3.3–5.3 MeV neutron energy region», Physical Review C 104, 044620 (2021)

[4] Haoyu Jiang, Zengqi Cui, Yiwei Hu, Jie Liu, Jinxiang Chen, Guohui Zhang, Yu. M. Gledenov, I. Chuprakov, E. Sansarbayar, G. Khuukhenkhuu, L. Krupa «Cross-section measurements for 58,60,61Ni(n, α)55,57,58Fe reactions in the 4.50 –5.50 MeV neutron energy region», Chinese Physics C, Vol. 44. No. 11 (2020)